E-Journal of Advanced Maintenance Vol. 13 No. 1 (2021) 12-20
Japan Society of Maintenology

A Novel Simulation Method of Thermal Cycle in Multi-pass Welding Process by Temper Bead Technique

Lina YU[1,*], Kazuyoshi SAIDA[1], Masahito MOCHIZUKI[1], Kazutoshi NISHIMOTO[4] and Naoki CHIGUSA[2]

[1] *Osaka University, 2-1 Yamadaoka, Suita, Osaka 565-0871, Japan*
[2] *The Kansai Electric Power Co., Inc., 8 Yokota, 13 Goichi, Mihama-cho, Mikata-gun, Fukui 919-1141, Japan*

ABSTRACT

Temper bead welding technique has been developed as one of effective repair method for pressurized water reactor, in case that post weld heat treatment (PWHT) is difficult to carry out. It is essential to confirm the tempering effect on the mechanical properties, and the appropriate welding conditions in temper bead welding needs to be predicted before the actual welding. Therefore, in this study, a novel numerical simulation method was proposed for predicting the temperature distribution and thermal cycle during multi-pass welding process by temper bead technique. As the results, the temperature distribution, such as A_{c1} line and weld metal line, were in good agreement between simulated and experimental results. Furthermore, based on the simulated thermal cycles the hardness distribution in heat affected zone (HAZ) was calculated, and the calculated hardness was in good accordance with the experimentally measured result. It follows that the currently proposed simulation method is effective for estimating the tempering effect during temper bead welding prior to actual welding.

KEYWORDS

Temper bead welding, Simulation model, FEM, Temperature distribution, Hardness

Article history:
Received October 2020
Accepted May 2021

ARTICLE INFORMATION

1. Introduction

Low alloy steel ASTM A533B possessing the superior low-temperature toughness and weldability is widely used to build pressurized water reactor vessels in nuclear power plants. However, the excellent mechanical properties of the base metal will be altered by the thermal cycles imposed by welding processes, and the increase in hardness and the loss of toughness always occur in the heat affected zone of the welds [1]. Therefore, post weld heat treatment (PWHT) is normally required to recover the toughness, eliminate the residual stress and reduce the hardness. However, PWHT is sometimes difficult to perform in operation in the case of repairing for large-scale structures. In practice, the temper bead welding technique is an effective repair welding method instead of PWHT [1-3]. Temper bead welding is a kind of multi-pass welding, in which the tempering effect is caused by heat-arising from the subsequent multi-layer weld thermal cycles. And it is essential to confirm the tempering effect on the mechanical properties and the appropriate welding conditions needs to be predicted prior to the actual welding.

To achieve the required tempering effect during temper bead welding, it is very important to predict the proper thermal cycle in multi-pass welding. Therefore, it is desired to develop a simple and useful numerical simulation method with the help of computer. Using the traditional simulation method [4-6], in order to prepare the simulation model, it is necessary to get the detailed information of the welding cross section after the actual welding. Therefore, the simulation model is difficult to complete prior to the actual multi-pass welding, and it takes a lot of time to create the complicated multi-pass welding model, especially difficult for the case for more than 100 pass welding. Therefore, a simple and quick simulation method without the detailed information of the welding cross section after the actual welding is expected to establish prior to the actual welding. In this study, a novel simply numerical simulation method was proposed for predicting the temperature distribution and thermal cycle during multi-pass welding process by temper bead technique, based on the single-pass bead shape database.

* Corresponding author, E-mail: yulina@mapse.osaka-u.ac.jp

And the simulated temperature distribution was compared with the experimental result to confirm the effectivity of the proposed simulation method. Furthermore, based on the simulated thermal cycles the hardness distribution in heat affected zone was predicted, which was also compared with the experimentally measured hardness to verify the effectivity of the newly proposed simulation method.

2. Materials and experimental procedures

The chemical compositions of the base metal low-alloy steel A533B and filler material MG-S56X used were shown in Table 1. The chemical compositions of the filler material MG-S56X were similar to the base metal A533B.

The single-pass welded sample (100×35×150 mm, shown in Fig. 1) was produced by GTAW (Gas Tungsten Arc Welding) with the welding conditions shown in Table 2. As shown in Fig. 2, the 7 layer - 152 pass temper bead welding was performed using the consistent layer technique [7], with the welding conditions shown in Table 3. The section surface was cut from the single-pass welded sample, and the sectioned surfaces of 1-layer, 3-layer and 7-layer weldments were cut from the multi-pass welded sample. The Vickers hardness was measured in the cross sectional area of the specimens after polishing and etching with 3% nital solution. The Vickers hardness measurement was performed at a load of 9.8N for 20s. In order to simulate the actual repair welding, the thermal cycle in heat affected zone (HAZ) of the 7 layer-152 pass welded sample was calculated using the following finite element (FE) simulation method proposed.

Table 1 Chemical compositions of materials

Material	Chemical compositions (mass %)												
	C	Si	Mn	P	S	Ni	Cu	Cr	Mo	Ti	Al	Fe	Co
A533B (Base metal)	0.12	0.26	1.43	0.006	0.002	0.53	0.02	0.01	0.51	-	0.038	Bal.	-
MG-S56X (Filler metal)	0.06	0.43	1.51	0.006	0.005	0.89	0.03	0.04	0.35	0.09	0.01	Bal.	<0.01

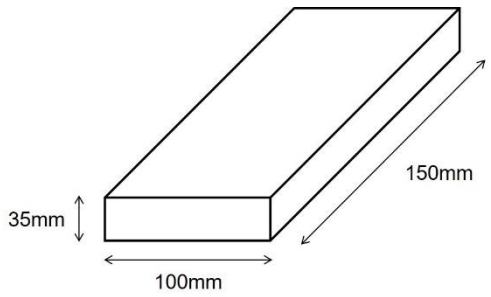

Fig. 1 Specimen for single-pass and multi-pass welding

Table 2 Welding conditions of single-pass welding

Welding condition	Current [A]	Voltage [V]	Wire sending [cm/min]	Welding speed [cm/min]	Heat input [J/cm]
①	250	16.7	200	10	25050
②	120	13.2	90	30	3168
③	200	15.2	160	30	6080
④	100	11.2	80	10	6720
⑤	200	15.7	150	20	9420
⑥	250	16.7	220	20	12525
⑦	140	13.2	110	30	3696
⑧	180	14.7	130	30	5292

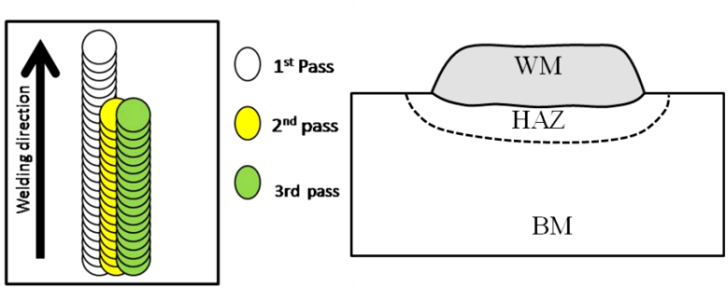

Fig. 2 Schematic illustration of temper bead welding

Table 3 Welding conditions of temper bead welding (7 layer-152 pass welding)

Layer	Current [A]	Voltage [V]	Wire feeding speed [cm/min]	Welding speed [cm/min]	Heat input [J/cm]	Number of passes
1st	250	16.7	200	10	25050	**12**
2nd	120	13.2	90	30	3168	**39**
3rd	140	13.2	110	30	3696	**30**
4th	200	15.2	160	30	6080	**23**
5th	200	15.7	150	20	9420	**16**
6th	200	15.7	150	20	9420	**16**
7th	200	15.7	150	20	9420	**16**

3. Novel simulation method for multi-pass welding

3.1 Bead shape database of single-pass welding

The single-pass welded sample was produced by GTAW with the welding conditions shown in Table 2. The section interface was cut from the center of the single-pass welded sample, and the cross sections of the single-pass welded sample were shown in Fig. 3. From the actual single-pass welded cross section, the information of bead width, height and depth for each single-pass welding condition has been collected as the database of weld bead shape and size for the novel FE simulation.

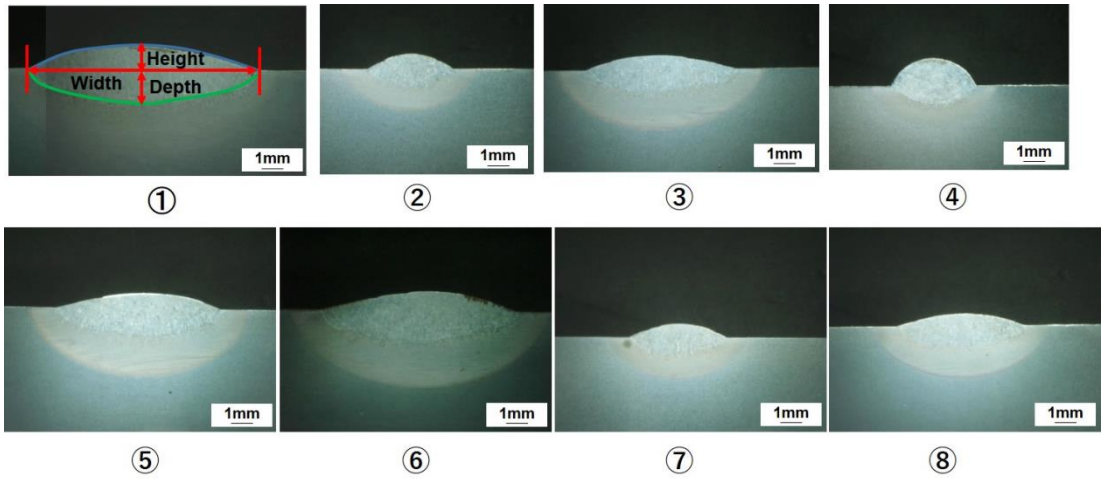

Fig. 3 Cross-sections of single-pass welded sample with different welding conditions

3.2 Concept of new simulation method

In the traditional simulation method, for example the simulation model as shown in Fig. 4, in order to prepare the simulation model, it was necessary to get the detailed information by taking the actual photographs of the welded cross-section of each layer after the actual welding. Therefore, the simulation model was difficult to complete prior to the actual multi-pass welding, and it took a lot of time to create the complicated multi-pass welding model, especially difficult for the multi-pass welded sample more than 100 pass welding as shown in Table 3. Therefore, a simple and quick simulation method without the detailed information of the welding cross section after the actual

welding is expected to develop prior to the actual welding.

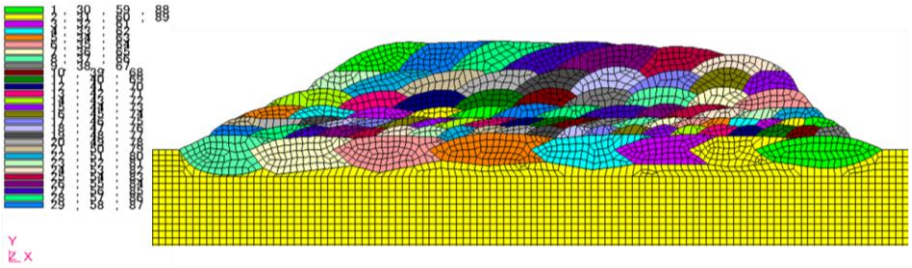

Fig. 4 Traditional simulation model for multi-pass welding

In this study, a novel simply simulation method was proposed, for predicting the temperature distribution and thermal cycle during multi-pass welding process by temper bead technique based on the obtained single-pass bead shape database, as shown in Fig. 5. According to the observed single-pass weld bead shape database, the heating range of each welding bead was automatically selected. The bead shape is consisted with two ellipses (up and down), and the element range fit the Equations (1) and (2) will be automatically selected as the heating part of the weld bead.

$$\frac{Y^2}{a_{up}^2}+\frac{Z^2}{b_{up}^2}<1 \tag{1}$$

$$\frac{Y^2}{a_{down}^2}+\frac{Z^2}{b_{down}^2}<1 \tag{2}$$

Where, *Y/Z* is the central coordinate of each weld bead, a_{up} is the half width of bead, b_{up} is the height of bead, a_{down} is the half width of bead, and b_{down} is the depth of bead.

Since the element range of each bead can be automatically selected, it is not necessary to create the material properties of each bead on creating the analysis model. And using this simulation method, the remelting between passes and the remelting between layers can be automatically considered in the simulation model, which is more close to the actual multi-pass welding. Furthermore, the model is easy to prepare, which can reduce the time for the simulation model creation, and the actual cross-sectional photographs of the sample are not needed, indicating that the simulation model can be prepared prior to the actual multi-pass welding.

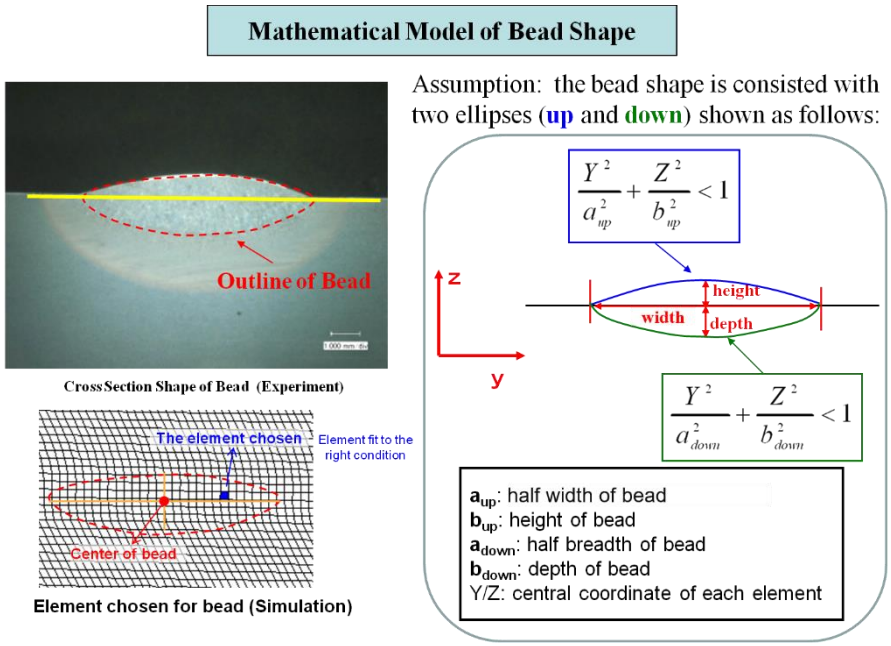

Fig. 5 Concept of the novel simulation method

4. FE simulation of temper bead welding and discussion

4.1 FE simulation model of temper bead welding

According to the novel proposed simulation method, the simulation model was also changed as shown in Fig. 6. There is only weld metal (WM) zone and base metal (BM) in the model. In order to select the bead shape more similar to the actual bead, the distance between the meshes of the WM part was set as 0.2 mm, which was finer than that of BM. And the distance between the meshes of the BM near WM was set to 0.5 mm, to easily analysis the thermal cycle in HAZ. As shown in the magnified part of Fig. 6, the heating range of each welding pass was automatically selected, based on the obtained single-pass bead shape database, according to the different welding conditions of every layer.

The temperature dependencies of physical properties of A533B are illustrated in Table 4. The welding conditions were the same as the experimental conditions shown in Table 3, which followed the consistent layer technique in temper bead welding.

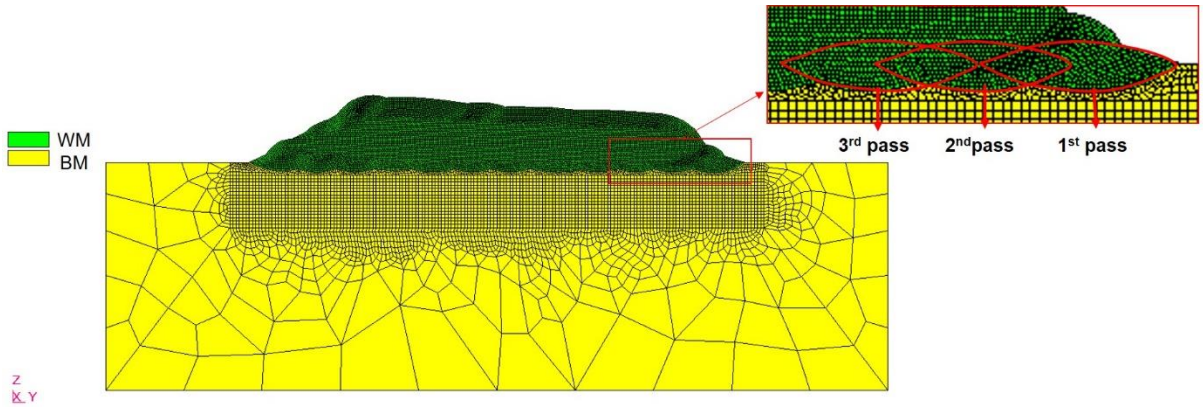

Fig. 6 Simulation model for 7 layer - 152 pass welding

Table 4 Temperature dependencies of material properties of A533B steel

Temperature (℃)	Specific heat (J/kg℃)	Thermal conductivity (W/mm℃)	Yield Strength (MPa)	Young's modulus (GPa)	Possion's ratio (-)	Thermal expansion (1/℃)
20	445	0.039	478	210	0.3	12.0e-6
200	517	0.0389	455	202	0.3	12.7e-6
400	592	0.036	405	188	0.3	13.9e-6
600	723	0.0317	238	160	0.3	13.8e-6
800	812	0.0378	75	115	0.3	12.6e-6
1000	658	0.0309	17	93	0.3	12.6e-6
1300	721	0.0365	5	10	0.3	14.5e-6

4.2 Temperature analysis of temper bead welding by FEM simulation

The temperature distributions produced by multi-pass thermal cycles in welds during temper bead welding were calculated using the novel proposed simulation method of the three-dimensional finite element analysis code, developed specifically for multi-pass welding simulation. Fig. 7 presents the calculated peak temperature distribution in the middle cross-section of 7 layer - 152 pass welds. The different peak temperatures are indicated by the different colors. The WM part was selected based on the previously obtained database of the single-pass bead shape, and WM range with peak temperature higher than the melting point of 1500 ℃ is shown in red color. And the region of HAZ are shown in rainbow colors according to the different peak temperatures.

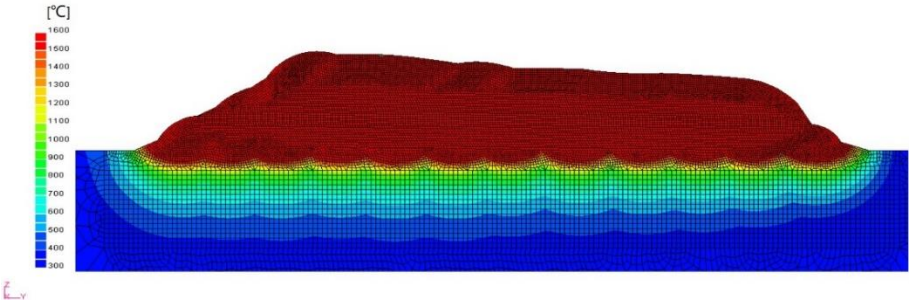

Fig. 7 Peak temperature distribution of 7 layer-152 pass welding

The region of the simulated WM with the maximum temperature higher than the melting point at the cross section was compared with the experimental result, as shown in Fig. 8. The height of WM region from the surface of the base metal were almost the same to the experimental result. And the A_{c1} line comparison between the simulated result and the experimental result was shown in Fig. 9. As the result of calculation, the deepest point of the A_{c1} line on the left side of multi-pass welding was 4.6 mm far from the sample surface, same to the actual welded cross sections, and the depth of the right side was 4.2 mm in both calculated result and experimental result. These facts indicated that the simulated temperature distribution agreed well with the experimental result.

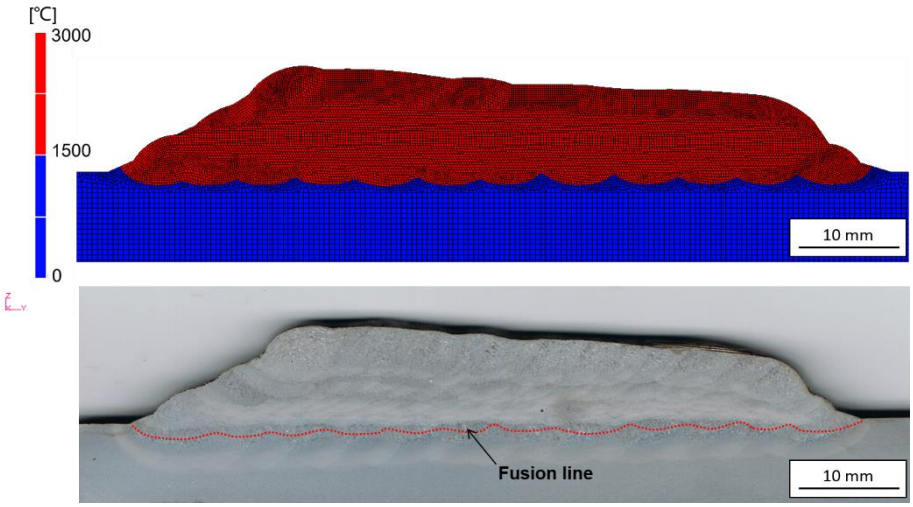

Fig. 8 Fusion line comparison of simulated result and the experimental result of 7 layer - 152 pass welding

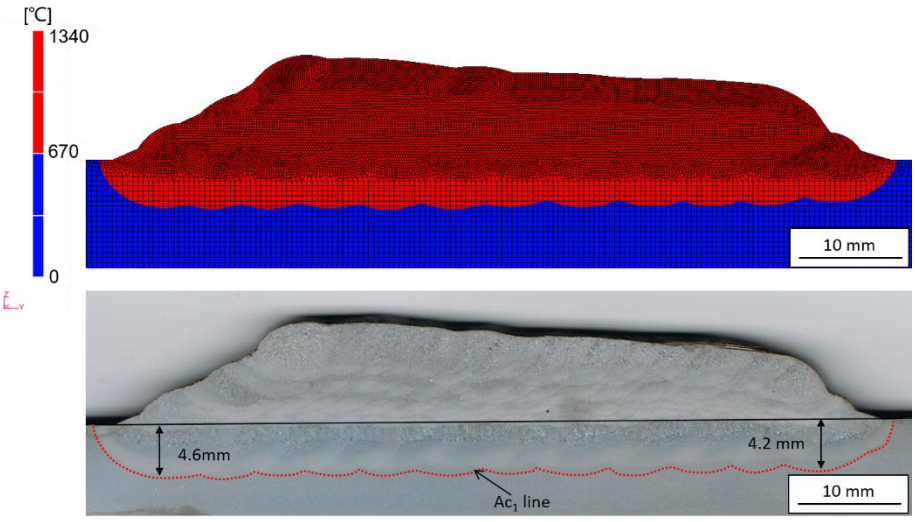

Fig. 9 Ac_1 line comparison of simulated result and the experimental result of 7 layer - 152 pass welding

4.3 Hardness prediction based on the simulated thermal cycles

Neural network (NN) [8,9] is a mathematical model or computational model that simulates the structure and/or functional aspects of biological neural networks. The NN-based hardness prediction system has been constructed previously based on the experimentally obtained hardness database by the authors [5]. According the thermal history at every grid node in HAZ, the simulated thermal cycle parameters (for example, T_p, CR) were fed into the proposed hardness prediction system, and the hardness at every grid node was calculated.

According the calculated hardness of every grid node, the visual hardness distribution in the HAZ after 1-layer welding, 3-layer welding and 7-layer welding were shown as color chart maps in Fig. 10 using the Mathematica software. Besides the red WM and grey BM regions, the hardness in the HAZ is shown with rainbow colors according to the different hardness levels. It could be found that after 1-layer welding as shown in Fig. 9 (a), there were some hardened zone with hardness higher than 350 HV appeared in the CGHAZ adjacent to the WM. However, after 3-layer and 7-layer temper bead welding as illustrated in Fig. 9 (b) and (c), the hardness in the whole HAZ was decreased and all values were lower than 350HV (the required specification in industry).

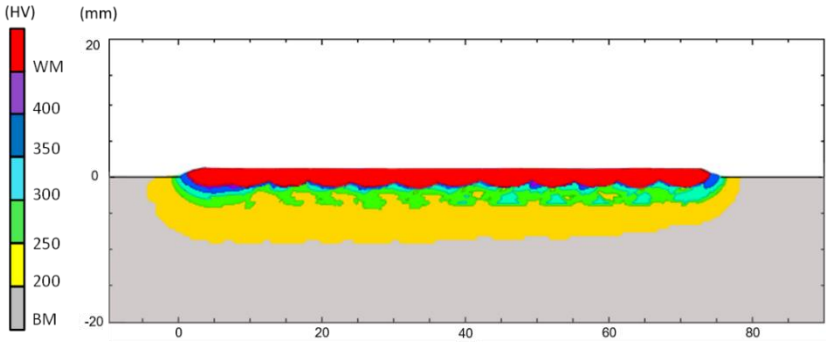

(a) 1 layer-12 pass welding

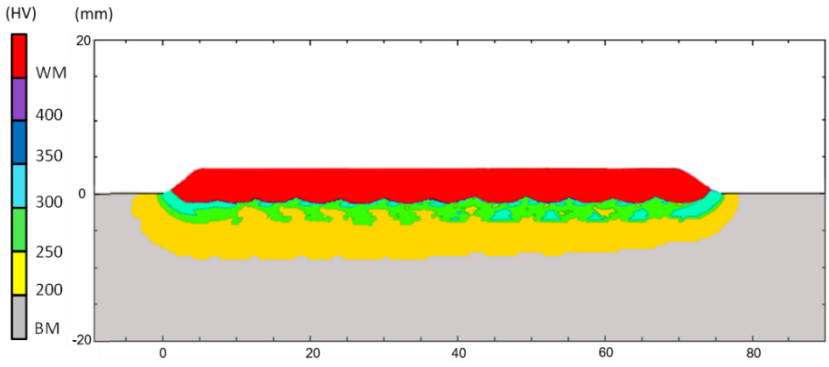

(b) 3 layer-81 pass welding

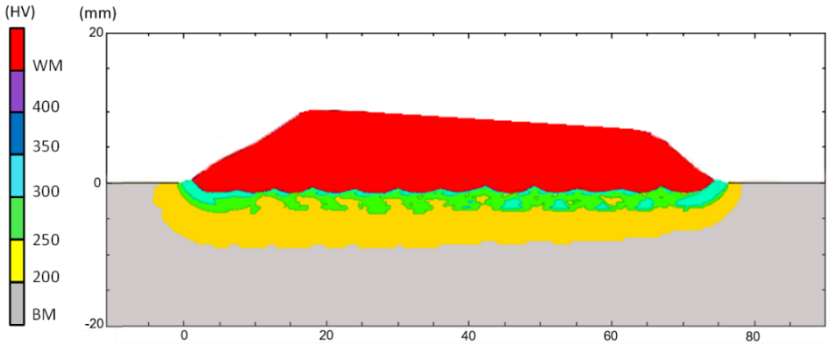

(c) 7 layer-152 pass welding

Fig. 10 Calculated hardness distribution of 7 layer-152 pass welding

The predicted hardness was compared with the experimentally measured results for the HAZ of A533B low-alloy steel after 7 layer - 152 pass welding, as shown in Fig. 11. The predicted and

measured values were performed along the yellow dotted line 2.5 mm far from the surface of the base metal, and the measurement distance of hardness was 1 mm. The red points were the experimentally measured hardness, and the blues points were the calculated hardness using the neural network-based hardness prediction system, based on the FE simulated thermal cycle. The predicted hardness was in good accordance with the experimentally measured hardness, and both the predicted and the measured hardness were lower than 350HV (the required specification in industry) after 3-layer and 7-layer temper bead welding. It follows that the proposed simple simulated method for multi-pass welding is useful and effective for estimating the tempering effect in temper bead welding.

It can be concluded that using the proposed simple simulation method, the hardness in HAZ is successfully predicted prior to the actual temper bead welding based on the FE simulated thermal cycle. If the calculated hardness in HAZ is higher than 350HV (it means it cannot fit the required specification in industry), the welding conditions would be modified. Thus, the appropriate welding conditions can be selected prior to the actual welding. The present novel simulation method is greatly useful and effective for the repair welding for the large structures.

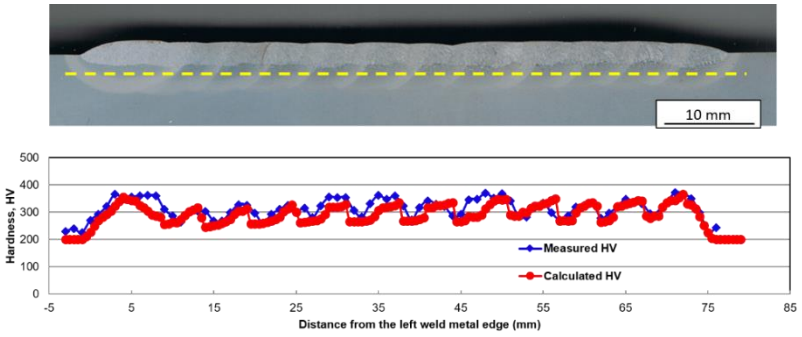

(a)1 layer-12 pass welding

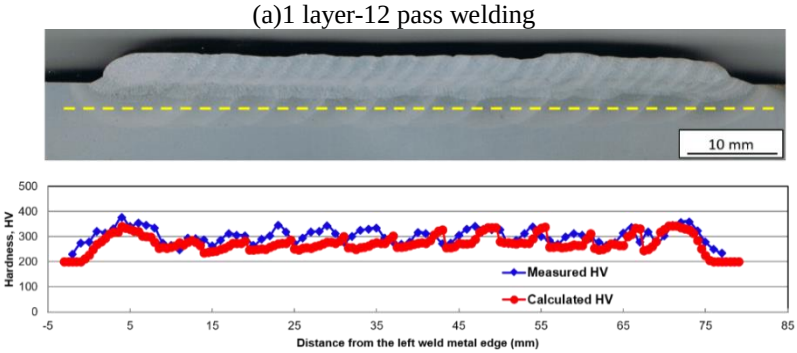

(b) 3 layer-81 pass welding

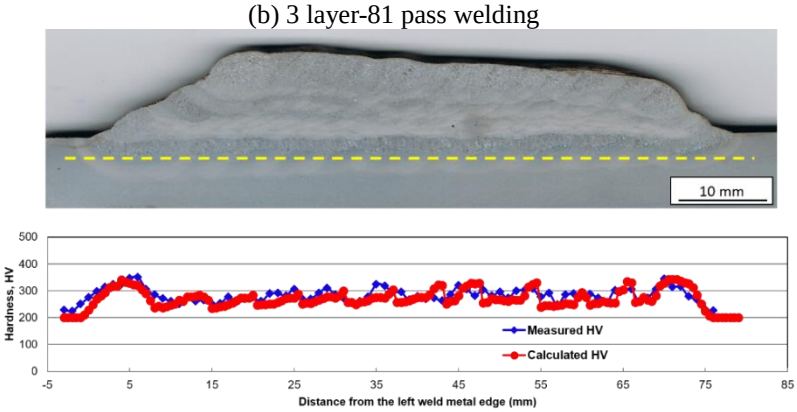

(c) 7 layer-152 pass welding

Fig. 11 Comparison of calculated hardness and measured hardness

5. Conclusions

(1) In order to simplify the FEM thermal cycle analysis, a novel numerical simulation method was proposed for predicting the temperature distribution and thermal cycle of temper bead welding,

based on the obtained bead shape database.

(2) The thermal history in HAZ of 7 layer - 152 pass welding by the consistent layer temper bead technique was simulated using the proposed method. As the results, the temperature distribution, such as A_{c1} line and weld metal line, was in good agreement between simulated and experimental results.

(3) Based on the simulated thermal cycle, the hardness distribution in HAZ was predicted, and the calculated hardness was in good accordance with the experimentally measured result. It followed that the proposed simulation method was greatly useful and effective for estimating the tempering effect during temper bead welding prior to actual welding.

References

[1] N. Yurioka, Y. Horii: "Recent developments in repair welding technologies in Japan", Science and Technology of Welding & Joining, Vol.11, pp. 255-264 (2006).

[2] J. Liao, K. Ikeuchi, F. Matsuda: "Toughness Investigation on Simulated Weld HAZs of SQV-2A Pressure Vessel Steel", Nuclear Engineering and Design, Vol.183, pp. 9-20 (1998).

[3] Y. Nakao, H. Ohige, S. Noi, Y. Nishi: "Distribution of Toughness in HAZ of Multi-Pass Welded High Strength Steel", Quarterly Journal of the Japan Welding Society, Vol.3, pp. 773-781 (1985).

[4] D. Deng, H. Murakawa, M. Shibahara: "Investigations on welding distortion in an asymmetrical curved block by means of numerical simulation technology and experimental method", Computational Materials Science, Vol.48, pp.187-194 (2010).

[5] L. Yu, Y. Nakabayashi, M. SaSa, S. Itoh, M. Kameyama, S. Hirano, N. Chigusa, K. Saida, M. Mochizuki and K. Nishimoto: "Neural network prediction of hardness in HAZ of temper bead welding using the proposed thermal cycle tempering parameter (TCTP)", ISIJ International, Vol.51, pp.1506-1515 (2011).

[6] L. Yu, M. SaSa, K. Ohnishi, M. Kameyama, S. Hirano, N. Chigusa, T. Sera, K. Saida, M. Mochizuki and K. Nishimoto: "Neural network-based toughness prediction in HAZ of low-alloy steel produced by temper bead welding repair technology", Science and Technology of Welding and Joining, Vol.18, pp. 120-134 (2013).

[7] R. Viswanathan, D. W. Gandy, S. J. Findlan: "Temper Bead Welding of P-Nos. 4 and 5 Materials", EPRI TR-111757, Final Report, December (1998).

[8] V. D. Manvatkar, A. Arora, A. De, T. DebRoy: "Neural network models of peak temperature, torque, traverse force, bending stress and maximum shear stress during friction stir welding", Science and Technology of Welding & Joining, Vol.17 , pp. 460-466 (2012).

[9] D. Casasent, X. Chen: "Radial basis function neural networks for nonlinear Fisher discrimination and Neyman-Pearson classification", Neural Networks, Vol.16, pp. 529-535 (2003).